

# Predicting Target Feature Configuration of Non-stationary Objects for Grasping with Image-Based Visual Servoing

Jesse Haviland<sup>1</sup>, Feras Dayoub<sup>1</sup>, Peter Corke<sup>1</sup>

**Abstract**—In this paper we consider the problem of the final approach stage of closed-loop grasping where RGB-D cameras are no longer able to provide valid depth information. This is essential for grasping non-stationary objects; a situation where current robotic grasping controllers fail. We predict the image-plane coordinates of observed image features at the final grasp pose and use image-based visual servoing to guide the robot to that pose. Image-based visual servoing is a well established control technique that moves a camera in 3D space so as to drive the image-plane feature configuration to some goal state. In previous works the goal feature configuration is assumed to be known but for some applications this may not be feasible, if for example the motion is being performed for the first time with respect to a scene. Our proposed method provides robustness with respect to scene motion during the final phase of grasping as well as to errors in the robot kinematic control. We provide experimental results in the context of dynamic closed-loop grasping.

## I. INTRODUCTION

Autonomous and reliable grasping is crucial to robots being able to complete useful tasks in the real world. This includes being able to operate in unstructured environments while grasping items that have never been previously seen. A robust robotic grasper must have the ability to operate in dynamic scenes where objects may be moving while being robust to errors in robotic actuation or error in sensor measurements.

To grasp robustly, with respect to dynamic scenes or sensor/actuation error, a closed-loop approach is required with the ability to perform grasp synthesis at a sufficient rate to use in the control loop. For example, the system [1], which is used in this work, can provide a grasp point in just 19ms given an RGB-D image of the scene. However, all RGB-D cameras have a minimum sensing distance for range data, typically in the order of 30cm. This minimum sensing distance is visualized in Figure 1. For objects closer than this “standoff” distance the camera provides an intensity image but not a range image. This leads to the problem of a 3D dependent control scheme becoming open-loop at the bounds of the camera. Monocular cameras, while having a focal length, do not suffer from these fundamental lower limits of the range, and can generally operate reliably at close range.

In order to perform closed-loop control after the minimum sensing distance of RGB-D cameras, a visual servoing (VS)

<sup>1</sup>Jesse Haviland, Feras Dayoub, and Peter Corke are with the Australian Centre for Robotic Vision (ACRV), Queensland University of Technology (QUT), Brisbane, Australia [j.haviland@qut.edu.au](mailto:j.haviland@qut.edu.au), [feras.dayoub@qut.edu.au](mailto:feras.dayoub@qut.edu.au), [peter.corke@qut.edu.au](mailto:peter.corke@qut.edu.au). This research was conducted by the Australian Research Council project number CE14100016.

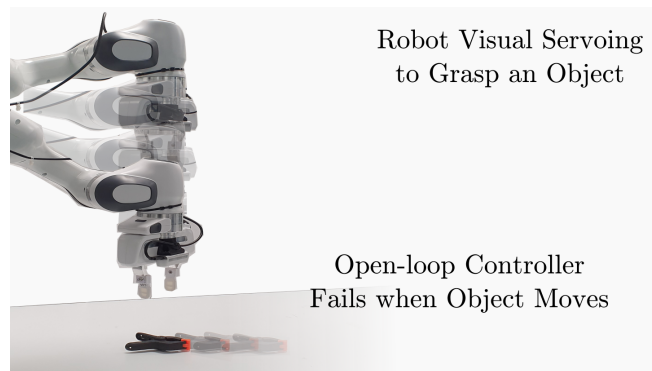


Fig. 1: We consider the problem of closed-loop grasping of non-stationary objects, in particular the final approach phase where depth information is no longer available from an RGB-D sensor. We use image-based visual servoing for this motion phase and servo toward a feature configuration predicted from the last valid depth image.

scheme is usually used. Image-based visual servoing (IBVS) is a control approach that uses a set of image-plane visual features (point coordinates, parameters of lines or ellipses, or image moments [2], [3]) to guide a camera to a desired pose with respect to the scene [4], [5]. A particular advantage of IBVS, compared to other VS schemes [4], for point-coordinate features is that the points are driven in straight lines on the image-plane and never leave the field of view.

IBVS is simple and remarkably robust but in practice there are three challenges. **Firstly**, the control law requires knowledge of the depth of the points. Fortunately IBVS is quite tolerant to errors in this depth estimate but the depth can also be estimated during the IBVS motion [6], [7]. **Secondly**, we need to determine the correspondence between the currently observed and goal image features. This can be achieved by using artificial features that are coded by size, shape or color. Alternatively a correspondence-free approach can be used [8]. **Thirdly**, the goal configuration of the image features is assumed to be known. If servoing with respect to a known model we can use visual geometry to determine the goal feature configuration. Alternatively, we can learn this configuration by moving the camera to the desired pose and record the feature configuration. However, we have a problem if there is no prior model or we do not have the opportunity to visit the scene in advance.

Addressing the three aforementioned challenges, in this paper we use IBVS to control the final approach phase of a dynamic grasper when depth information is no longer available from the RGB-D sensor. We assume that the camera

has good depth-of-field and is able to form a sharply focused RGB image at close range.

The contributions of this paper are:

- 1) a novel method to predict the goal image-feature configuration from RGB images of the scene.
- 2) a novel switching controller that uses IBVS to guide the final approach phase of a dynamic closed-loop grasping system which enables a closed-loop controller to operate to the completion of the grasp.
- 3) experimental validation for dynamic scenes.

## II. RELATED WORK

**Nomenclature** We use the notation of [9] where  $\{x\}$  denotes a coordinate frame,  ${}^xP \in \mathbb{R}^3$  is a point in 3D space defined with respect to the coordinate frame  $\{x\}$ ,  ${}^x p \in \mathbb{R}^2$  is an image-plane point with respect to the coordinate frame  $\{x\}$ , and  ${}^y\xi_x$  is a relative pose or rigid-body transformation, of  $\{x\}$  with respect to  $\{y\}$ .

### A. Using a Feature Detector for Visual Servoing

Using a feature detector to define image plane points for an IBVS scheme is a popular choice for robots operating in un-engineered environments. Feature detection and matching involves: features (or interest points), and feature descriptors. The more prevalent features include: SIFT features [10], SURF features [11], and the MSER region features [12]. A study including five major feature descriptors evaluated SIFT descriptors [10] as being the best in all categories other than luminance changes [13].

In many VS controllers, unique features need to be matched between two separate images that have been taken from two different positions. To achieve this reliably, descriptors need to be generated for each feature which are invariant to scale, orientation, illumination, and affine transformations. Many approaches for finding matches between features exist, such as the ratio test proposed in [10] or using the fundamental matrix with Random Consensus Algorithm (RANSAC) [14].

One of the first methods of utilizing features for VS uses feature matches to define epipolar geometry between two scenes [15]. Epipolar geometry can recover the relative angular motion of the camera and translation (only up to an unknown scale) given enough matched points in the image through the essential matrix (for general scenes), or a homography matrix (for a planar scenes) [16]. The approach depends on knowing the scene of the desired camera pose, and assumed the translational scale to recover the relative translation of the camera.

A subsequent approach proposed a new method of identifying robust SIFT features to more reliably calculate feature matches [17]. This approach uses the known camera pose between scenes to maintain a database of features based on feature similarity, keypoint orientation, and epipolar consistency. The approach also assumes that the desired scene is known and uses matched features between this scene and the current scene of the robot as the input to an IBVS scheme.

Other approaches exist which variously: experiment with image reference features with SIFT descriptors [18], use epipolar lines to define a sliding visual servoing scheme [19], applies IBVS on a mobile robot [20], and using SIFT features and descriptors with a known 3D model of the goal object to guide a position-based visual servoing (PBVS) scheme [21]. The approaches in [18], [19], and [20] depend on knowing the scene of the desired camera location, meaning all of the stated related work assumes that prior knowledge of the destination is known. This is a major issue, especially in the context of grasping never seen before objects, where prior knowledge is not available.

### B. Visual Servoing for Grasping

A key problem in robotic grasping is determining the grasp point. Grasp point synthesis is a well established field with many methods [22]–[24]. Recently, grasp point synthesizers using deep learning approaches have proven very successful, even on never-before-seen items and scenes [1], [25]–[27]. These synthesizers have been able to learn effective and important features present in depth images to output reliable grasp points.

Closed-loop grasping involves using a VS scheme to position the robot’s end-effector in such a way that it can grasp an object. The current state-of-the-art in robotic grasping uses a simple PBVS scheme to guide the end-effector to the grasp point [1], [25]–[27]. The error used in the PBVS controller is defined as  ${}^c\xi_{c^*}$  where  $\{c\}$  is the current camera pose, and  $\{c^*\}$  is the desired camera pose at the grasp point. However, these approaches rely on depth information from an RGB-D camera which has a minimum operating distance, which means the last stage of the grasp is completed in an open-loop manner.

## III. PROPOSED GRASP CONTROLLER

We propose a method predicting target feature point locations for an IBVS controller which eliminates the need for prior knowledge of the target scene. The method only needs initial depth information of the scene which allows it to work at ranges closer than any 3D sensor allows. We apply this approach to a switching visual servoing controller to achieve fully closed-loop robotic grasping. The proposed controller operates as follows:

- 1) Perform continuous grasp point detection while using PBVS to approach the goal, utilizing 3D information from an RGB-D camera. See Frame A in Figure 2.
- 2) At the lower limit of the depth camera’s range: lock in the grasp point and store the SIFT features, descriptors, and 3D locations of the RGB-D camera’s current view. See Frame B in Figure 2.
- 3) Match features in the camera’s view to the previously stored features using SIFT. Project the matched features into the camera’s image plane to form an IBVS control law. Finish the approach to the grasp goal using image plane point features and IBVS. See Frame C in Figure 2.
- 4) Grasp the object at the grasp point.

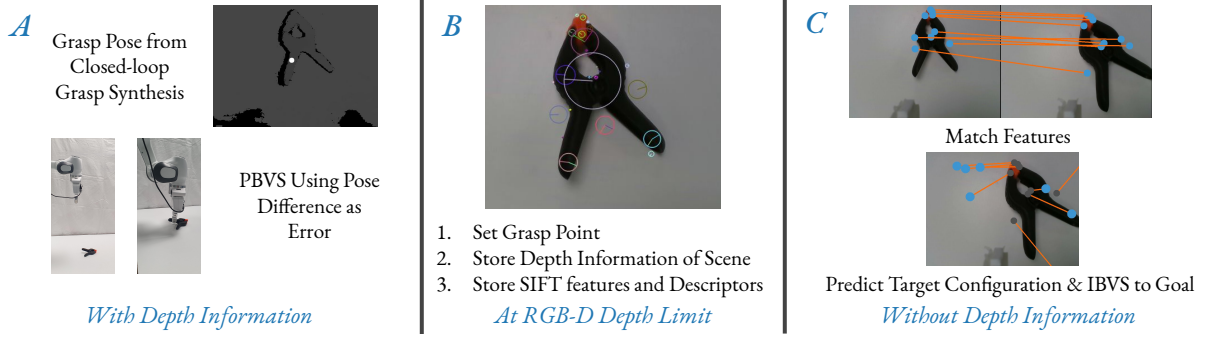


Fig. 2: Overview of proposed switching grasp controller. The robot continuously performs grasp point synthesis while using a PBVS scheme to approach the grasp point (shown in A). At the depth limit of the RGB-D camera the robot stores SIFT key points with locations of the current view of the scene, and set a grasp pose (shown in B). After this point, features in the current scene are matched to the stored information, before predicting the configuration of these features at the grasp point (shown in C).

Section IV describes our approach to determining the desired grasp pose before Section V details the proposed switching VS scheme. Section VI describes our experimental setup and methodology. Finally, Section VII details our experimental results and insights informed by the results.

#### IV. GRASP POSE CALCULATION

We are utilizing the grasp point synthesizer devised by Morisson et. al. [1]. This system, unlike competing deep learning approaches, provides a real time output (reported as 19 ms per image) making it suitable for a closed-loop system.

The grasp point synthesizer takes in a depth image  ${}^cI_d = \mathbb{R}^{H \times W}$  (where  $H$ , and  $W$  are the height and width of the image), and outputs a 2D array of grasps,  ${}^cI_g = \mathbb{R}^{H \times W}$  (one for each pixel in the input depth image). In  ${}^cI_g$ , a grasp is defined as

$$\mathbf{g} = (\mathbf{p}_s, \theta, w, q)$$

where  $\mathbf{p}_s = (u, v)$  is the image plane coordinate for an antipodal grasp (the grasp is executed perpendicular the the  $x$ - $y$  axis in the camera's reference frame),  $\theta$  is the grasp angle,  $w$  is the grasp width in image coordinates, and  $q$  is a scalar quantity used to measure the grasp quality.

If the camera's intrinsic parameters are known, 3D positions of depth values from the depth image can be calculated using the following

$${}^cP = \begin{pmatrix} X \\ Y \\ Z \end{pmatrix} = \begin{pmatrix} f_x & 0 & u_0 \\ 0 & f_y & v_0 \\ 0 & 0 & 1 \end{pmatrix}^{-1} \begin{pmatrix} u \\ v \\ z \end{pmatrix} \quad (1)$$

where  $(u, v)$  is the image plane coordinate of the depth value  $z$ ,  $(u_0, v_0)$  is the principle point of the camera,  $(f_x, f_y)$  is the focal length of the camera (measured in pixels), and  ${}^cP = (X, Y, Z)$  represents the 3D position. Using (1) a grasp  ${}^c g$  in image coordinates can be turned into

$$\mathbf{G} = ({}^c\mathbf{P}_s, {}^c\theta_y, W, q)$$

in the 3D coordinates of the camera's reference frame, where  ${}^c\mathbf{P}_s$  represents the 3D location of the grasp,  ${}^c\theta_y$  represents

the yaw angle of the grasp,  $W$  represents the grasp width in metres, and  $q$  represents the grasp quality.

The grasp point synthesizer can be defined as a function

$$M({}^cI_d) = {}^cI_G$$

where  ${}^cI_d$  is the input depth image and  ${}^cI_G$  is the output image of grasps. The best visible grasp is then

$$\mathbf{G}^* = \max_q {}^cI_G$$

When performing closed-loop calculation of  $\mathbf{G}^*$ , there is a potential for similar ranked grasps in multiple location of the image and thus  $\mathbf{G}^*$  may jump rapidly greatly in the image degrading the speed and quality of the VS controller. To counteract this, the previous  $\mathbf{G}^*$  is stored as  $\mathbf{G}_m$  and the next  $\mathbf{G}^*$  is defined as the closest (in image plane coordinates) of three peaks of the local maxima around  $\mathbf{G}_m$ .

The grasp pose in  $\{c\}$  can then be defined as  ${}^c\xi_g \in \mathbb{R}^6$  comprizing of cartesian position and roll, pitch, and yaw Euler angles

$${}^c\xi_g = \begin{pmatrix} {}^cP_{s_x} \\ {}^cP_{s_y} \\ {}^cP_{s_z} \\ 0 \\ 0 \\ {}^c\theta_y \end{pmatrix}$$

where roll and pitch angles are set to 0 as the grasp synthesizer outputs antipodal grasp positions. Note that this means that the  $\omega_r, \omega_p$  velocities can be set to 0 in the control law. This pose also represents the desired location of the end-effector;  ${}^c\xi_g = {}^c\xi_{e^*}$ .

Then, to get the pose between the initial  $\{c\}$  and desired camera location  $\{c^*\}$

$${}^c\xi_{c^*} = {}^c\xi_{e^*} \bullet {}^e\xi_c$$

where  ${}^e\xi_c$  is a static pose between the camera reference frame and the robot's end-effector reference frame.

## V. SWITCHING VS CONTROL SCHEME

We propose using a switching controller to exploit the benefits of both PBVS and IBVS while avoiding their major shortcomings. PBVS provides an optimal cartesian path to the goal but is prone to errors introduced from camera calibration and robot odometry. This makes PBVS best suited to getting the robot close to the goal. IBVS is very robust to sensor error but may produce sub-optimal cartesian paths. Therefore IBVS is best utilized in the final approach to the target. Figure 2 above demonstrates this approach.

### A. PBVS Controller

The PBVS controller is defined as

$$\mathbf{v} = \lambda({}^e\xi_g - {}^e\xi)$$

where  $\lambda \in \mathbb{R}^6$  is the gain for the controller, and  $\mathbf{v} \in \mathbb{R}^6$  is the cartesian velocity and roll, pitch and yaw Euler angles for the end-effector of the robot. This controller will run while the distance  ${}^cP_{s_x}$  (the distance from the camera to the grasp point) is greater than 25 cm. This is approximately the point at which 3D camera information will degrade.

### B. Switching to the IBVS Controller

The point at which the controllers switch is the last time 3D information can be collected. The camera frame at the current location is defined as  $\{c_1\}$ . The SIFT algorithm is run over the RGB image  ${}^{c_1}p_I$  to form a dictionary of reference features and descriptors  ${}^{c_1}p_f$ . Each entry in  ${}^{c_1}p_f$  has an associated 3D location in  ${}^{c_1}P_I$ .

### C. IBVS Controller

A typical IBVS scheme sets out guide a robot to a desired position within the image plane. This approach is generalized as the following

$$\mathbf{e}(t) = \mathbf{s} - \mathbf{s}^* \quad (2)$$

where  $\mathbf{s}$  is a set of image plane features and  $\mathbf{s}^*$  is a set of the desired feature locations in the image plane.

An interaction matrix (often referred to as the image Jacobian) is used to relate the two-dimensional velocity of a pixel in the image-plane to the three-dimensional velocity of the camera (which in turn is typically the end-effector of a robot) [4].

The equation which relates pixel velocity to camera velocity is

$$\mathbf{v}_p = \mathbf{J}_c \mathbf{v}_c \quad (3)$$

where  $\mathbf{v}_p \in \mathbb{R}^2$  is the pixel velocity,  $\mathbf{v}_c \in \mathbb{R}^6$  is the camera velocity, and  $\mathbf{J}_c \in \mathbb{R}^{2 \times 6}$  is the image Jacobian.  $\mathbf{J}_c$  in (3) extends to

$$\mathbf{J}_c = \begin{pmatrix} \frac{-f}{Z} & 0 & \frac{u}{Z} & \frac{uv}{-f} & \frac{-(f+u^2)}{f} & v \\ 0 & \frac{-f}{Z} & \frac{v}{Z} & \frac{f+v^2}{f} & \frac{-uv}{f} & -u \end{pmatrix} \quad (4)$$

where  $(u, v)$  is the pixel location in the image,  $f$  is the focal length (in pixel units), and  $Z$  is the depth value of the pixel (the distance from the camera's x-y plane to the pixels

corresponding point in the world). The image Jacobian for each feature point are stacked on top of each other such that the resulting Jacobian takes the form  $\mathbf{J} \in \mathbb{R}^{2n \times 6}$ , where  $n$  is the number of feature points.

Subsequent images,  ${}^{c'}p_I$ , are taken relative to the camera's new reference frame  $\{c'\}$ , without having access to any depth information. The SIFT algorithm is then used on the new image  ${}^{c'}p_I$  to produce a new set of features and descriptors denoted as  ${}^{c'}f$ .

Matches between  ${}^{c_1}p_f$  and  ${}^{c'}p_f$  are computed to produce set of matches  $\mathbf{M}$  such that an individual match  $\mathbf{m}$  is

$$\mathbf{m} = ({}^{c_1}p_m, {}^{c'}p_m, d)$$

where  ${}^{c_1}p_m$  is the image plane location of the feature in the  $\{c_1\}$  frame,  ${}^{c'}p_m$  is the image plane location of the feature in the  $\{c'\}$  frame, and  $d$  is a distance metric. Matches more likely to be errors are eliminated using the distance ratio test outlined in [10]. The IBVS controller works better when the target feature points are spread out around the image. To ensure this, a  $20 \times 20$  grid is placed over the image, where a maximum of one matched feature is kept per grid cell. To further reduce incorrect matches, the fundamental matrix is calculated using RANSAC. This produces a list of inlier, and outlier matches where only inlier matches are retained.

The velocity used to command the robot's end-effector is defined through manipulation of the relationship shown in (3)

$$\mathbf{v}_c = \mathbf{v}_e = -\lambda \mathbf{J}^+ \mathbf{e} \quad (5)$$

Where  $\mathbf{v}_e \in \mathbb{R}^6$  is the spacial velocity of the robot's end-effector,  $\lambda$  is the gain of the controller,  $\mathbf{J}^+ \in \mathbb{R}^{6 \times 2n}$  is the Moore-Penrose pseudo inverse of the stacked image Jacobian from (4),  $\mathbf{e} \in \mathbb{R}^{2n}$  is the error vector from (2), and  $n \in \mathbb{Z} \geq 4$  is the number target feature points.

### D. Grasping

When the error calculated in (2) gets sufficiently small, the servoing is considered complete and a grasp can be attempted. This is completed by instructing the grippers on the robot to close. The robot then retreats upwards before dropping the object to the side of the grasping scene.

## VI. EXPERIMENTS

We validate and evaluate our approach through testing on an arm-type robot. Our approach is realized using ROS middleware and primarily Python code. Our experiments first seek to validate that the approach works given near ideal conditions, before evaluating the robustness and consistency on repeated grasping trials.

### A. Equipment

All experiments are performed using the Franka-Emika Panda robot, equipped with 3D-printed grippers using a design from [28]. We use an Intel RealSense D435 camera to provide RGB and depth information, which is mounted to the robot's end-effector.

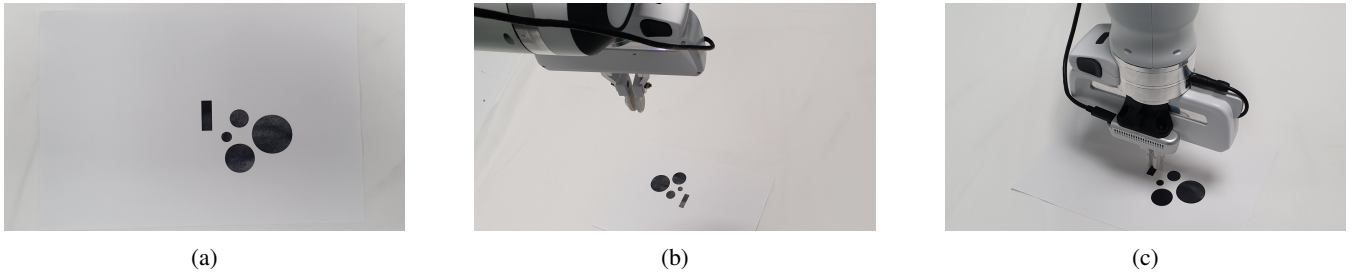


Fig. 3: (a) The target features printed on A4 paper. (b) The robot’s position before attempting to reach the goal. (c) the robot in the goal state.

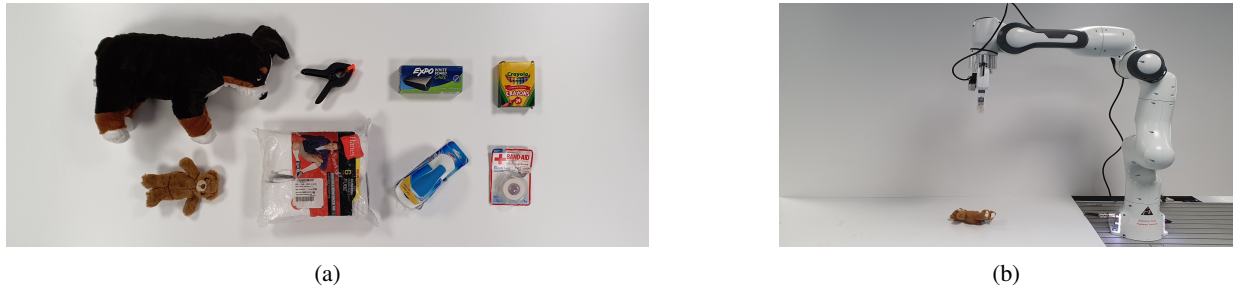


Fig. 4: (a) The 8 household objects which are to be grasped. (b) The robot’s position before attempting a grasp.

### B. Experiment 1: Predicting Target Feature Configuration

We first validate our target feature configuration predictor through an IBVS controller with both static and dynamic targets. These tests seek to demonstrate that the target feature configuration can be predicted using only initial depth information, and operate in a closed-loop controller.

In these tests the goal consists of a known shape with a distinguishable orientation. The robot is trying place its end-effector at this goal. Along with the goal position, there are also target features which will constitute points in the control system. These features are known shapes which are easily distinguishable from each other and easy to register between view points. This is visualized in Figure 3c. The target features are printed on an A4 piece of paper with a set of target features as seen in Figure 3a.

In the static test, the robot is initialized 40 cm above a table, with the target having a random orientation located within the camera’s field of view. Such a position is shown in Figure 3b. In the dynamic tests, the target feature points are moved in a random translational motion such that they remain visible to the camera.

### C. Experiment 2: Grasping Trials

We then evaluate our switching visual servoing scheme on grasping tasks. We perform dynamic grasping trials on common household objects, where the object on the table is moved in a random fashion while the robot attempts to grasp it. The target objects are displayed in Figure 4a. The objects vary in size, and grasp difficulty. In this test, one of the objects is randomly placed on a table located within a  $30 \times 30$ cm square. The robot then attempts to grasp the object 10 times, from a set starting position, and place it in a bin to the side of the table. The starting configuration of the robot

with an object is displayed in Figure 4b. The robot attempts 10 grasps per object.

## VII. RESULTS

The results from the static test with known features show that, given perfect registration between features, the approach will allow the robot to achieve the goal. Figure 5 shows the average feature error between each feature point and the desired location of that feature point in the image plane. Figure 7b displays the path the features took in the image plane. This shows a typical path of an IBVS controller, where features aim make a straight line towards the goal. Figure 7a displays the initial view of the features from the camera’s point of view. This Figure also shows the desired feature configuration as calculated by our algorithm and the ideal IBVS path to approach this configuration.

The results from the dynamic test with known features verifies that the controller can operate with dynamic scenes. Figure 5 displays the target feature error. The large spikes show when the target features are moved in the scene. However, the figure shows that the controller recovers from these disturbances and achieves the goal.

Figure 6 displays the target feature point error in a static and dynamic object grasp attempt. This shows that there is more noise present in the system when using SIFT features than with known features (see Figure 5), however, the system still reaches the goal.

Results from the repeated dynamic grasping trials are displayed in Table I. These results show that our approach is viable for dynamic grasping tasks. The performance of the system was stronger on larger objects and objects which had many unique SIFT features. This is as our approach relies on numerous unique features being present in the scene

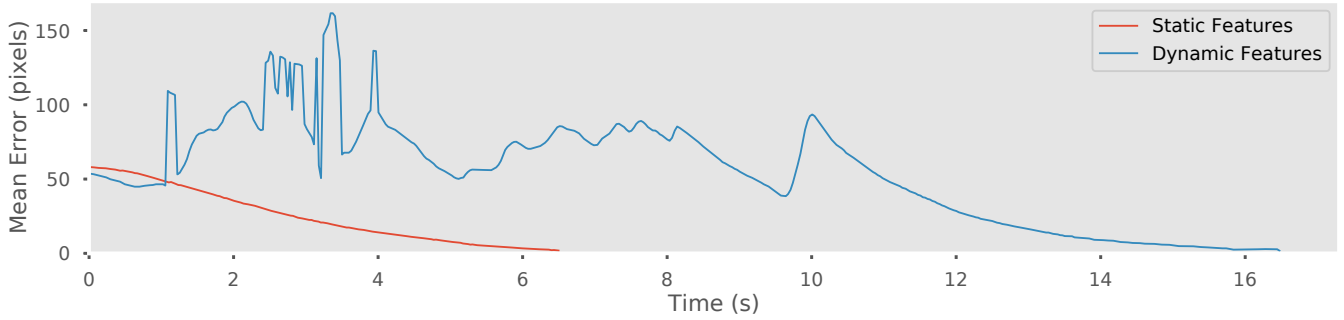


Fig. 5: Target Feature Error in Static and Dynamic Test with Known Features

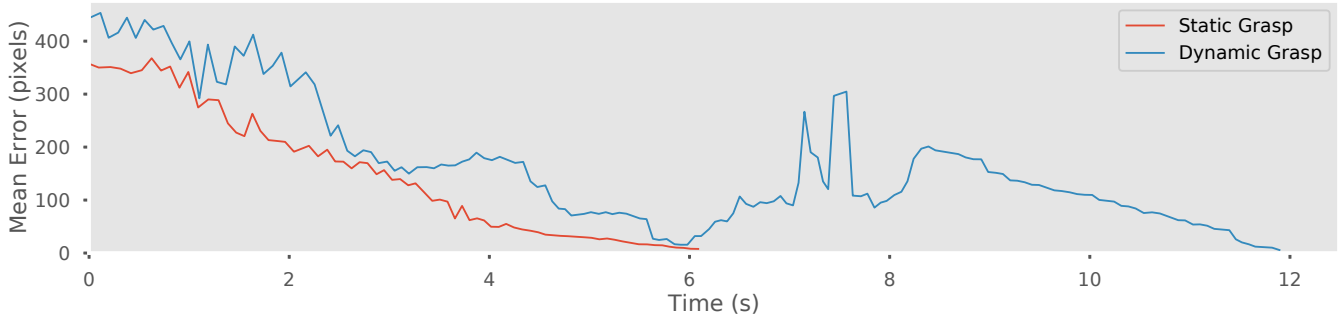


Fig. 6: Target Feature Error in a Static and Dynamic Grasping Trial

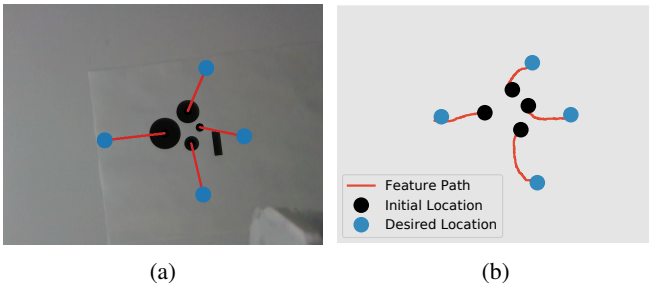


Fig. 7: Static Test with Known Features (a) Photo of Initial and Desired Feature Configuration from the Initial Camera POV. (b) Actual Target Feature Trajectory in the Image Plane.

with enough remaining to being visible to the camera at the grasp point. This limits the types of scenes and objects our approach will reliably work on. This could be mitigated through developing a new method of collection features such as using lines, object shapes, or image moments. An alternate method of mitigating this issue is to use a feature rich background such as a tablecloth underneath the objects.

TABLE I: Experimental Results From Grasping Trials

	Grasp Rate in [1]
Static Objects	92%
Dynamic Objects	0%
Using our Approach with Dynamic Objects	<b>76.25%</b>

Our approach relies on feature matching which has inherent flaws. Image features are not as accurate or reliable as depth information from an RGB-D camera. Therefore, in static scenes with stationary objects, a pure PBVS controller, such as in [1], will provide better results.

Our approach is designed to extend and improve upon the state-of-the-art in robotic grasping such as [1], to be able to work in dynamic environments where objects are non-stationary. The current state-of-the-art in grasping relies on 3D information, which is limited by the minimum distance required to sense depth information. At this limit, the controllers go open-loop and will fail if there is a disturbance to the object. Consequently, the success rate of these controllers for fully dynamic scenes is 0%.

The results in Table I shows that our dynamic grasping success rate is 76.25%. Therefore, our approach significantly advances and improves upon the state-of-the-art in grasping in the context of fully dynamic scenes.

## VIII. CONCLUSIONS

In this paper we have considered the problem of closed-loop grasping of dynamic scenes, and in particular the final approach phase where depth information is no longer available from an RGB-D sensor. We use image-based visual servoing for this motion phase and servo toward a feature configuration predicted from the last valid depth image. This is in contrast to most previous IBVS work where the goal feature configuration is assumed to be known. We have demonstrated the robustness of the approach in the context of dynamic closed-loop grasping.

## REFERENCES

- [1] D. Morrison, J. Leitner, and P. Corke, "Closing the loop for robotic grasping: A real-time, generative grasp synthesis approach," in *Robotics: Science and Systems XIV*. Robotics: Science and Systems Foundation, June 2018.
- [2] F. Chaumette, "Image moments: a general and useful set of features for visual servoing," *IEEE Transactions on Robotics*, vol. 20, no. 4, pp. 713–723, Aug 2004.
- [3] F. Chaumette and S. Hutchinson, "Visual servo control. II. Advanced approaches [Tutorial]," *IEEE Robotics Automation Magazine*, vol. 14, no. 1, pp. 109–118, March 2007.
- [4] S. Hutchinson, G. D. Hager, and P. I. Corke, "A tutorial on visual servo control," *IEEE Transactions on Robotics and Automation*, vol. 12, no. 5, pp. 651–670, Oct 1996.
- [5] F. Chaumette and S. Hutchinson, "Visual servo control. I. Basic approaches," *IEEE Robotics Automation Magazine*, vol. 13, no. 4, pp. 82–90, Dec 2006.
- [6] J. T. Feddema and O. R. Mitchell, "Vision-guided servoing with feature-based trajectory generation (for robots)," *IEEE Transactions on Robotics and Automation*, vol. 5, no. 5, pp. 691–700, Oct 1989.
- [7] N. P. Papanikolopoulos and P. K. Khosla, "Adaptive robotic visual tracking: theory and experiments," *IEEE Transactions on Automatic Control*, vol. 38, no. 3, pp. 429–445, March 1993.
- [8] A. McFadyen, J. Ford, and P. Corke, "Stable image-based visual servoing with unknown point feature correspondence," in *2017 IEEE 56th Annual Conference on Decision and Control (CDC)*, Dec 2017, pp. 4278–4282.
- [9] P. Corke, *Robotics, Vision and Control*, 2nd ed. Springer International Publishing, 2017.
- [10] D. G. Lowe, "Distinctive Image Features from Scale-Invariant Keypoints," *International Journal of Computer Vision*, vol. 60, no. 2, p. 91110, Nov 2004.
- [11] H. Bay, T. Tuytelaars, and L. Van Gool, "SURF: Speeded Up Robust Features," in *Computer Vision ECCV 2006*, A. Leonardis, H. Bischof, and A. Pinz, Eds. Berlin, Heidelberg: Springer Berlin Heidelberg, 2006, p. 404417.
- [12] J. Matas, O. Chum, M. Urban, and T. Pajdla, "Robust wide baseline stereo from maximally stable extremal regions," *Image and Vision Computing*, vol. 22, pp. 761–767, 09 2004.
- [13] K. Mikolajczyk and C. Schmid, "A performance evaluation of local descriptors," *IEEE Trans. Pattern Anal. Mach. Intell.*, vol. 27, no. 10, pp. 1615–1630, Oct. 2005.
- [14] M. A. Fischler and R. C. Bolles, "Random sample consensus: A paradigm for model fitting with applications to image analysis and automated cartography," *Commun. ACM*, vol. 24, pp. 381–395, 1981.
- [15] A. Shademan and F. Janabi-Sharifi, "Using scale-invariant feature points in visual servoing," in *SPIE Optics East*, 2004.
- [16] Y. Ma, S. Soatto, J. Košecká, and S. S. Sastry, *An Invitation to 3-D Vision*. Springer New York, 2004.
- [17] F. Hoffmann, T. Nierobisch, T. Seyffarth, and G. Rudolph, "Visual servoing with moments of sift features," in *2006 IEEE International Conference on Systems, Man and Cybernetics*, vol. 5, Oct 2006, pp. 4262–4267.
- [18] A. Maxim, C. Lazar, A. Burlacu, and C. Copot, "Robotic visual servoing system based on sift features," in *2012 16th International Conference on System Theory, Control and Computing (ICSTCC)*, Oct 2012, pp. 1–6.
- [19] J. Xin, B. Ran, and X. Ma, "Robot visual sliding mode servoing using sift features," in *2016 35th Chinese Control Conference (CCC)*, July 2016, pp. 4723–4729.
- [20] H. Lang, Y. Wang, and W. d. S. Clarence, "Vision based object identification and tracking for mobile robot visual servo control," in *IEEE ICCA 2010*, June 2010, pp. 92–96.
- [21] F. Liefhebber and J. Sijs, "Vision-based control of the manus using sift," in *2007 IEEE 10th International Conference on Rehabilitation Robotics*, June 2007, pp. 854–861.
- [22] A. Bicchi and V. Kumar, "Robotic grasping and contact: a review," in *Proceedings 2000 ICRA. Millennium Conference. IEEE International Conference on Robotics and Automation. Symposia Proceedings (Cat. No.00CH37065)*, vol. 1, April 2000, pp. 348–353 vol.1.
- [23] A. Sahbani, S. El-Khoury, and P. Bidaud, "An overview of 3d object grasp synthesis algorithms," *Robot. Auton. Syst.*, vol. 60, no. 3, pp. 326–336, Mar. 2012. [Online]. Available: <http://dx.doi.org/10.1016/j.robot.2011.07.016>
- [24] K. Shimoga, "Robot Grasp Synthesis Algorithms: A Survey," *The International Journal of Robotics Research*, vol. 15, no. 3, p. 230266, 1996. [Online]. Available: <https://doi.org/10.1177/027836499601500302>
- [25] E. Johns, S. Leutenegger, and A. J. Davison, "Deep learning a grasp function for grasping under gripper pose uncertainty," in *2016 IEEE/RSJ International Conference on Intelligent Robots and Systems (IROS)*, Oct 2016, pp. 4461–4468.
- [26] I. Lenz, H. Lee, and A. Saxena, "Deep learning for detecting robotic grasps," *The International Journal of Robotics Research*, vol. 34, no. 4-5, p. 705724, 2015. [Online]. Available: <https://doi.org/10.1177/0278364914549607>
- [27] J. Mahler, J. Liang, S. Niyaz, M. Laskey, R. Doan, X. Liu, J. Aparicio, and K. Goldberg, "Dex-net 2.0: Deep learning to plan robust grasps with synthetic point clouds and analytic grasp metrics," in *Robotics: Science and Systems XIII*. Robotics: Science and Systems Foundation, July 2017.
- [28] M. Guo, D. V. Gealy, J. Liang, J. Mahler, A. Goncalves, S. McKinley, J. A. Ojea, and K. Goldberg, "Design of parallel-jaw gripper tip surfaces for robust grasping," in *2017 IEEE International Conference on Robotics and Automation (ICRA)*, May 2017, pp. 2831–2838.